energies

MDPI

Article

Decoupled Speed and Flux Control of Three-Phase PMSM Based on the Proportional-Resonant Control Method

Haneen Ghanayem *, Mohammad Alathamneh and R. M. Nelms

Electrical and Computer Engineering Department, Auburn University, Auburn, AL 36849, USA
* Correspondence: hig0002@auburn.edu

Abstract: Field-oriented control (FOC) has achieved great success in permanent magnet synchronous motor (PMSM) control. For the PMSM drive, FOC allows the motor torque and flux to be controlled separately, which means the torque and flux are decoupled from each other. Since the torque control is achieved by the speed controller, it can be considered that the speed and the flux of the PMSM are also decoupled from each other and can be controlled separately. In this paper, we propose a PMSM vector control using decoupled speed and flux controllers based on the proportional-resonant (PR) control method. A flux controller is proposed to control the flux of the PMSM and generate the d-axis reference current, whereas the speed regulator is used to generate the torque as well as the q-axis reference current. The PR controller is proposed to control the dq-axis currents and generate the reference voltages; its design is included.Therefore, decoupled speed and flux controllers are controlled separately using the PR controller. The Matlab/Simulink environment is utilized for the simulation, while the dSPACE DS1104 is used for the experimental work. The proposed control method is simple; there are no flux or torque estimators required, so it can avoid the complexity of estimators in the control scheme. The motor is tested under different scenarios, including flux change, speed change, and load torque change. The simulation and hardware results show the effectiveness of the proposed control method in controlling the the speed and the flux of PMSM with fast motor response and good dynamic performance in the different scenarios.

Keywords: decoupled control; flux controller; PMSM; proportional-resonant; speed control; vector control

Citation: Ghanayem, H.; Alathamneh, M.; Nelms, R.M. Decoupled Speed and Flux Control of Three-Phase PMSM Based on the Proportional-Resonant Control Method. *Energies* **2023**, *16*, 1053. https://doi.org/10.3390/en16031053

Academic Editor: Adolfo Dannier

Received: 15 December 2022
Revised: 10 January 2023
Accepted: 13 January 2023
Published: 18 January 2023

1. Introduction

Nowadays, permanent magnet synchronous motors (PMSMs) are widely recommended for many industrial applications due to their simple structure, high performance, excellent efficiency, and high reliability [1]. Field-oriented control (FOC), also called vector control (VC), is the most common technique used to control the PMSM. The FOC method allows the motor torque and flux to be controlled separately, which means the torque and flux are decoupled from each other. Moreover, direct torque control (DTC), voltage vector control (VVC), and non-linear control are classified under vector control techniques [2–4]. Figure 1 presents the flowchart of the PMSM control techniques.

In [5], the authors propose a PMSM based on FOC and DTC control strategies using the space vector pulse width modulation (SVPWM) technique. To apply the FOC scheme, a mechanical sensor was required to determine the motor position. On the other hand, flux and torque estimators were required to achieve the DTC technique. In [6,7], the authors compared FOC and DTC techniques in controlling the PMSM. The performance of each method was included. The simulation results showed that the FOC scheme has a fast speed response and low torque ripple. On the other hand, the switching frequency based on the DTC scheme is much lower than the FOC scheme. In [8], the authors proposed a DTC speed control of PMSM based on a fractional PID controller method. Compared to a traditional PID controller, better motor performance was achieved. In [9], the authors

presented PMSM performance based on the DTC technique using a SVPWM inverter. A torque and flux linkage estimator was required to apply the DTC scheme. The proposed control method achieved fast dynamic performance with low ripple in the torque and the speed response.

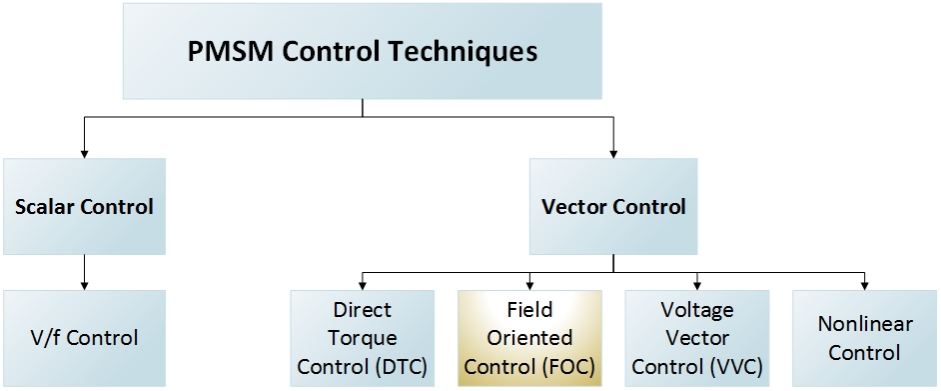

Figure 1. PMSM control techniques diagram.

In [10], the authors proposed a speed control of a PMSM based on the current model predictive controller (MPC). The proposed control method was compared with the traditional vector control methods, such as FOC and DTC techniques. The simulation and the experimental results showed that the MPC method improved the overall performance of the PMSM.

A robust nonlinear predictive current control (RNPCC) for a PMSM is described in [11]. Compared to traditional predictive current control (PCC), the RNPCC has strong robustness and good dynamic performance. In addition, the current error, which was caused by a parameter disturbance, was removed.

A model predictive speed control (MPC) for a three-phase PMSM was discussed in [12]. Based on the MPC controller, the overshoot, the settling time, and the overall performance of the PMSM were improved. In [13], the authors proposed a double MPC to control the speed and the current of the PMSM. The MPC controller was used for the speed outer loop, while the deadbeat predictive controller was used for the current inner loop. The proposed control strategy proves its efficacy in controlling the PMSM with no overshoot, excellent steady-state performance, and fast speed response.

Speed control of the PMSM based on a sliding mode controller was studied in [14]. The sliding mode controller was designed for the speed loop, while the PI controller was used to control the current of the PMSM. Excellent static and dynamic speed performances were achieved.

A disturbance compensation based on model predictive flux control (DCB-MPFC) of a surface permanent magnetic synchronous motor (SPMSM) with optimal duty cycle (ODC) using a two-level inverter is discussed in [15]. The proposed method was compared to the PI model predictive torque control (PI-MPTC) method. The simulation and the experimental results validated the effectiveness of the proposed control method in reducing the torque ripple as well as its ability to reject the torque disturbance.

In [16], the authors present a novel direct instantaneous torque and flux control of the PMSM with an adaptive linear neuron (ADALINE)-base motor model. Based on the proposed control method, the torque ripples were cancelled, and the parameter sensitivity was eliminated. The simulation results showed the fast and smooth torque response of the PMSM as well as the robustness of the proposed control method against the disturbance and the parameter variations.

Reference [17] proposed a new deadbeat direct current controller of PMSM based on two adjacent voltage vectors: the active voltage vectors (AVVs) and the zero voltage vector (ZVV). The proposed method improved the motor performance. The torque and the flux

ripple were reduced, the THD stator current was decreased, and a fast dynamic response was obtained.

References [18–21] presented a deadbeat direct torque and flux control of PMSM (DB-DTFC). Six-Phase PMSM torque control was used in [22] by injecting a fifth-harmonic into each phase current of the stator. In [23], a deadbeat current and flux vector control(DB-CFVC) of interior permanent magnet synchronous motor (IPMSM) was presented. The stator flux linkage vector was implemented in $\alpha\beta$ stationary coordinates instead of rotating frame (dq coordinates).

Vector control of a PMSM based on the proportional resonance (PR) control method was described in [24]. The simulation results illustrated a comparison in motor performance between the PI controller and the PR control method. The proposed control method was simple to implement and improved the overall performance of the PMSM.

An active disturbance rejection control for speed variation suppression of the PMSM using a proportional resonant (PR-ADRC) controller was discussed in [25]. The PR-ADCR control method was proposed to eliminate speed variation due to any internal or external disturbance. In addition, the PR controller was combined with the linear extended state observer (LESO), and with this combination, the dc and ac disturbances of the speed loop were totally rejected.

Reference [26] presented a speed estimator for direct torque and flux control (DTFC) of PMSM using model reference adaptive control (MRAC) based on rotor flux. The reference model represents the voltage model, while the adaptive model represents the current model. The proposed method was tested with and without load disturbance; therefore, the simulation results showed that the speed estimate followed the reference speed exactly and the ripples in the torque and current response were reduced.

The authors in [27] presented a stator flux linkage adaptive SVM-DTC control strategy for a PMSM. The stator flux adaptive algorithm was used to control the dq-axis currents through the MTPA method. Comparing the stator flux linkage adaptive SVM-DTC control method with the traditional SVM-DTC, the simulation results validated the efficacy of the proposed control method in reducing the stator output current, which significantly improved the control of the motor.

In this paper, a vector control technique for a PMSM using decoupled flux and speed controllers based on a PR current controller is proposed. The d-axis reference current (i_d^*) is no longer kept at zero; therefore, a separate flux controller is used to achieve the d-axis reference current. On the other hand, the speed controller is used to achieve the q-axis reference current of the PMSM. In addition, the PR controller was designed for the inner current loop to control the dq-axis reference currents and generate the dq-axis reference voltages. The speed and the angular position of the PMSM can be measured using the motor encoder. The actual flux and torque of the PMSM are determined directly using simple calculations; therefore, no flux or torque estimator is required.

The novel contributions of this work are as follows:

- The speed and flux decoupled controllers are proposed to control the dq-axis current through the PR controller.
- Both speed and flux control are achieved separately.
- The PR controller is proposed to control the dq-axis currents and generate the reference voltages.
- This method does not require a phase-locked loop (PLL), which makes it simpler.
- No flux or torque observer is required, which makes the overall control strategy less complex.

The organization of the paper is as follows: Section 1 discusses the introduction and the literature review, and Section 2 includes the mathematical model of the PMSM. Section 3 analyzes the proposed control method. Section 4 provides system simulation results. Section 5 presents the test setup platform with the experimental results. Section 6 summarizes the conclusion.

2. The Mathematical Model of PMSM

The model of the PMSM can be presented in the *abc* domain or the two-axis *dq* domain. However, the *dq* model has been widely used due to its simplicity in the motor control. The voltage equations of the PMSM are given in Equations (1) and (2).

$$V_d = R_s i_d + L_d \frac{di_d}{dt} - \omega_r L_q i_q \tag{1}$$

$$V_q = R_s i_q + L_q \frac{di_q}{dt} - \omega_r (L_d i_d + \psi_m) \tag{2}$$

The PMSM flux equations are shown in Equations (3) and (4), while Equation (5) describes the permanent magnet flux linkage.

$$\psi_{sd} = L_d i_d + \psi_m \tag{3}$$

$$\psi_{sq} = L_q i_q \tag{4}$$

$$\psi_m = \frac{1}{\sqrt{3}} \frac{K_e}{1000p} \frac{60}{\pi} \tag{5}$$

The developed torque of the PMSM is given in Equation (6). For a surface mounted PMSM, $L_d = L_q$, and the torque equation can be rewritten as in Equation (7).

$$T_e = \frac{3}{2} p(\psi_m i_q + (L_d - L_q) i_d i_q) \tag{6}$$

$$T_e = \frac{3}{2} p(\psi_m i_q) = K_t i_q \tag{7}$$

The relation between the rotor electrical speed and the rotor mechanical speed of the PMSM is described as in Equation (8).

$$\omega_m = \omega_e \frac{2}{p} \tag{8}$$

In order to convert the voltages and the current from *abc* to *dq*0 reference frame, park transformation [28] is utilized as shown in Equations (9) and (10).

$$\begin{bmatrix} V_d \\ V_q \\ V_0 \end{bmatrix} = \frac{2}{3} \begin{bmatrix} sin(\theta_r) & sin(\theta_r - 120) & sin(\theta_r + 120) \\ cos(\theta_r) & cos(\theta_r - 120) & cos(\theta_r + 120) \\ \frac{1}{2} & \frac{1}{2} & \frac{1}{2} \end{bmatrix} \begin{bmatrix} V_a \\ V_b \\ V_c \end{bmatrix} \tag{9}$$

$$\begin{bmatrix} V_a \\ V_b \\ V_c \end{bmatrix} = \begin{bmatrix} sin(\theta_r) & cos(\theta_r) & 1 \\ sin(\theta_r - 120) & cos(\theta_r - 120) & 1 \\ sin(\theta_r + 120) & cos(\theta_r + 120) & 1 \end{bmatrix} \begin{bmatrix} V_d \\ V_q \\ V_0 \end{bmatrix} \tag{10}$$

Park to Clarke transformation (*dq*0 to $\alpha\beta$0 transformation) [28] can be applied based on Equations (11) and (12).

$$\begin{bmatrix} V_\alpha \\ V_\beta \\ V_0 \end{bmatrix} = \begin{bmatrix} cos(\theta_r) & -sin(\theta_r) & 0 \\ sin(\theta_r) & cos(\theta_r) & 0 \\ 0 & 0 & 1 \end{bmatrix} \begin{bmatrix} V_d \\ V_q \\ V_0 \end{bmatrix} \tag{11}$$

$$\begin{bmatrix} V_d \\ V_q \\ V_0 \end{bmatrix} = \begin{bmatrix} sin(\theta_r) & -cos(\theta_r) & 0 \\ cos(\theta_r) & sin(\theta_r) & 0 \\ 0 & 0 & 1 \end{bmatrix} \begin{bmatrix} V_\alpha \\ V_\beta \\ V_0 \end{bmatrix} \tag{12}$$

3. Control Algorithm Description

A speed/flux decoupling technique based on the FOC scheme using the PR controller method is proposed. The FOC method allows the motor torque and flux to be controlled separately, which means the torque and flux are decoupled from each other. The speed controller is a proportional-integral (PI) regulator, which produces the reference torque. The calculated torque is compared with the reference torque, generating the torque error signal. Then, the q-axis reference current (i_q^*) is generated based on the constant relationship between the torque and the q-axis reference current as shown in Equation (7). Since the d-axis reference current (i_d^*) is not zero, a flux controller is proposed. The flux controller is based on a PI regulator. The calculated flux is compared with the reference flux generating the error signal of the d-axis reference current (i_d^*). Furthermore, the proportional resonant (PR) controller is suggested for the inner current loop. However, to apply the PR control method, Park's inverse transformation ($dq/\alpha\beta$) is required. Then, the inverter is controlled by pulse width modulation (PWM). The block diagram of the proposed control method is shown in Figure 2.

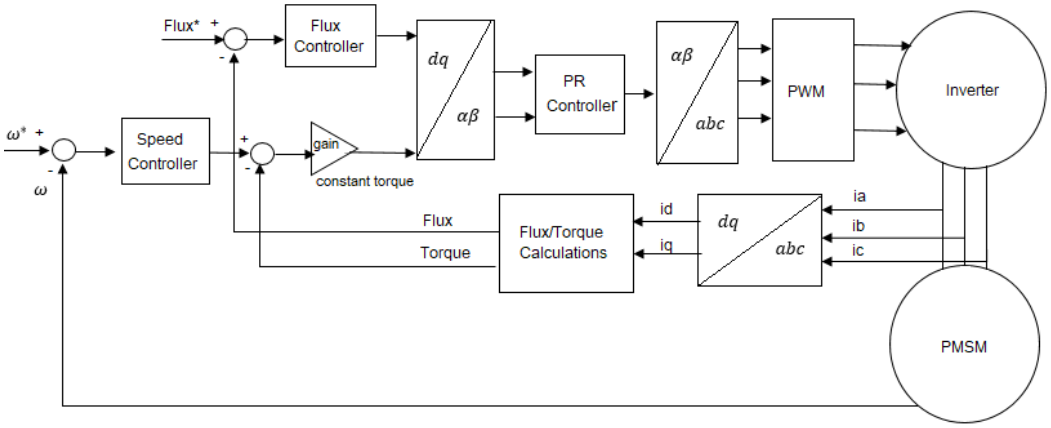

Figure 2. Block diagram of the proposed method.

3.1. The Speed and Flux Controllers Design Using PI Controller

The speed and the flux controllers are constructed based on the PI controller. The gains of the PI controller are designed based on Ziegler–Nichol's (ZN) method [1,29].

The transfer function of the PI- controller is described in Equation (13).

$$G_{PI}(s) = K_P + \frac{K_i}{s} \tag{13}$$

Based on ZN's method, K_i and K_P are adjusted to satisfy Equations (14) and (15).

$$K_p = 0.45K_{cr} \tag{14}$$

$$K_i = \frac{1.2K_p}{P_{cr}} \tag{15}$$

where K_{cr} is a critical point gain, andP_{cr} is the corresponding period of sustained oscillation.

3.2. The Current Controller Design Using a PR Controller

The current controller is constructed based on the PR control method. The principle of the PR controller is to eliminate the steady-state error by introducing an infinite gain at a fundamental sinusoidal signal [30]. The transfer function of the PR controller is given by Equation (16).

$$G_{PR}(s) = K_p + K_r \frac{s}{s^2 + \omega^2} \tag{16}$$

where K_p and K_r are the proportional and the resonant control gains, respectively, and ω is the fundamental angular frequency.

Here, ω can be chosen at the desired reference current frequency or the fundamental frequency at $\omega = 2\pi f = 2\pi(60) = 377\frac{\text{rad}}{\text{s}}$. The controller gains ($K_p$ and K_r) can be tuned using [30,31] as follows:

- The main target of the PR controller is to make the measured current equal to the reference current; in other words, make the error equal to zero.
- The gain K_r is first set to zero.
- K_p can be increased from zero until sustained oscillations in the error waveform occur at $K_{p,cr}$.
- Set $K_p = 0.45K_{p,cr}$.
- The value of K_r can be increased from 0 until a zero steady-state error occurred.
- Note that a larger value can help to eliminate the steady-state error and reduce the settling time, but it creates a larger overshoot. There is a trade-off between steady-state error and overshoot. Choose the suitable value of K_r for your desired overshoot and settling time.

4. PMSM Performance Analysis and Simulation Results

4.1. Motor Specifications, Controller Design, and Simulation Model

The performance of the three-phase PMSM using decoupled speed and flux controller based on the PR control method is examined using the Matlab/Simulink environment. The motor specifications are listed in Table 1.

Table 1. PMSM specifications.

Parameter	Value
Rated power	200 W
Rated voltage	42 V
Max speed	3000 RPM
Pole-pairs number	4
Voltage constant	9.5 V/Krpm
Resistance (L-L)	0.4 Ohms
Inductance (L-L)	540 µH
Magnetic flux linkage	0.01309 Wb

The current response overshoot was assumed to be 5%, and the settling time was selected as 3 s. Then, based on the tuning rules in Section 3, the PR gains can be found.

The Simulink model of the closed loop PR controller and the current error signal is shown in Figure 3. The error signal waveform shows that the controller behaviour is following the desired characteristic. The speed, flux, and current controller gains are listed in Table 2.

Table 2. Controller gains.

	Speed	Flux	Currents
Controller gains	$K_p = 2.5$ $K_i = 0.5$	$K_p = 0.2$ $K_i = 1.09$	$K_p = 0.5$ $K_r = 32$

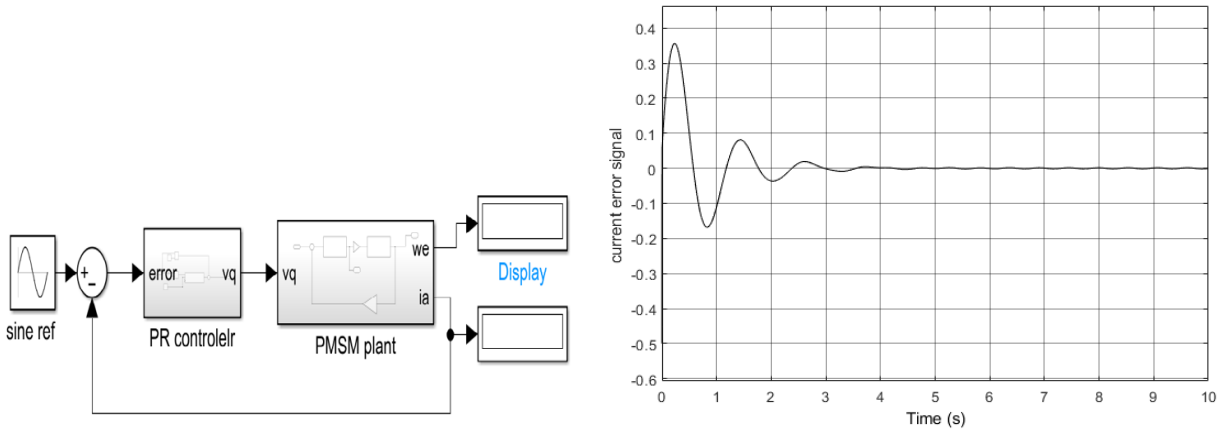

Figure 3. Simulink model of the closed loop PR controller and current error signal waveform for the selected gains.

The Simulink model of the PMSM using decoupled flux and speed controller based on the PR control method is depicted in Figure 4.

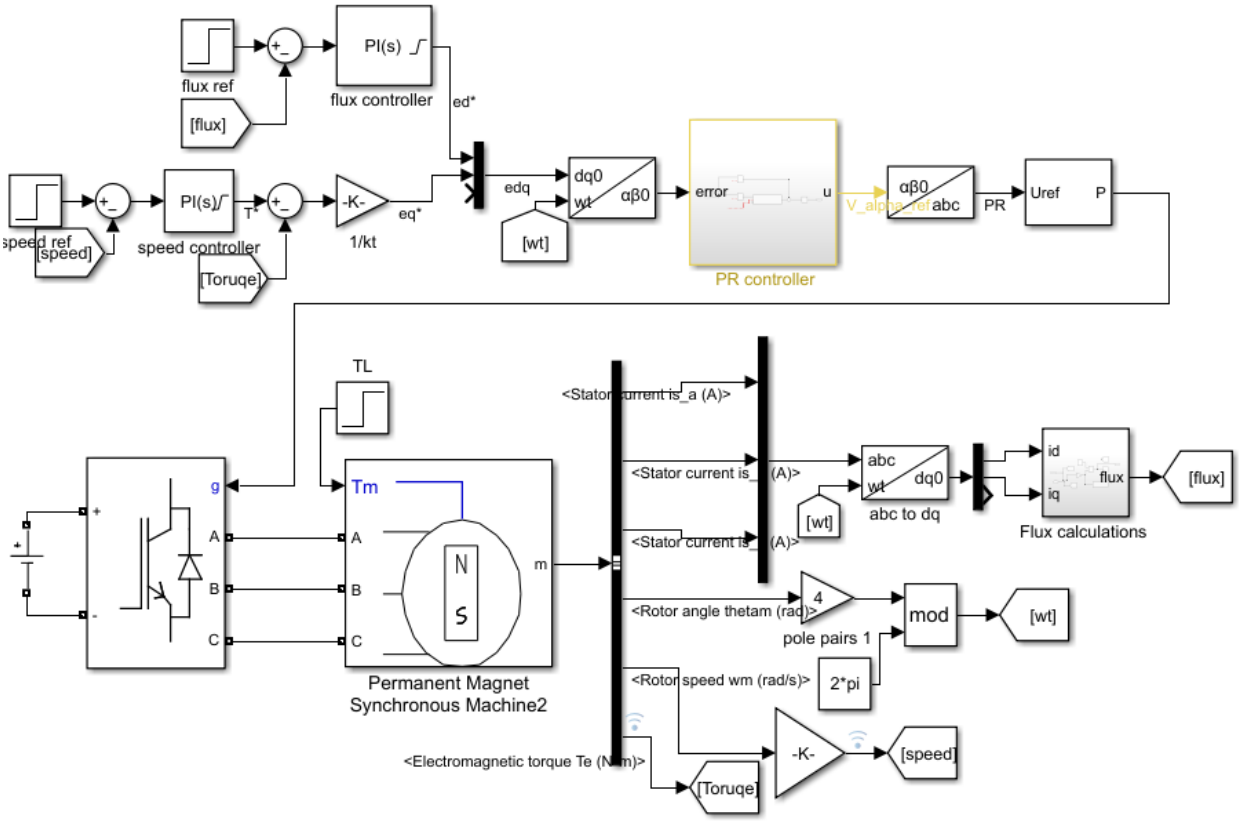

Figure 4. The Simulink model using the proposed control method.

4.2. PMSM Simulation Performance

The simulation model was built using Matlab/Simulink and was run for 2 s. The reference speed, the reference flux, and the load torque were applied to the PMSM as a step input and are shown in Equations (17), (18), and (19), respectively.

$$\omega_{ref} = \begin{cases} 300 \text{ rpm}, & 0 < t < 1 \\ 500 \text{ rpm}, & 1 < t < 2 \end{cases} \quad (17)$$

$$Flux_{ref} = \begin{cases} 0.5 \text{ Wb}, & 0 < t < 0.5 \\ 1 \text{ Wb}, & 0.5 < t < 2 \end{cases} \tag{18}$$

$$T_L = \begin{cases} 0.1 \text{ N.m.}, & 0 < t < 1.5 \\ 0.3 \text{ N.m.}, & 1.5 < t < 2 \end{cases} \tag{19}$$

The overall performance of the PMSM is shown in Figure 5. The reference flux was increased to 1 Wb at $t = 0.5$ s. The flux controller kept the actual flux as its reference value. The d-axis current i_d was increased to 2 A. The speed reference was changed to 500 rpm at $t = 1$ s, and as shown in the results, the speed regulator keeps the PMSM speed as its reference value. In addition, the load torque was increased to 0.3 N.m at $t = 1.5$ s. With the load change, the speed and the flux are still kept as their reference, while the q-axis current i_q increased to 4 A.

Figure 6 presents the transient response of the electromagnetic torque, flux, and the dq-axis currents. The first transient for all quantities occurred at the motor startup around $t = 0.41$ s. Figure 6a presents the transient response for the electromagnetic torque, the second transient occurred when the reference speed changed at $t = 1$ s, and the third transient occurred at $t = 1.5$ s when the load torque was changed. Figure 6b presents the flux transient response and the second transient at $t = 0.5$ s when the flux reference was changed. It can be seen that the flux response was not affected by the reference speed change at $t = 1$ s. Figure 6c,d present the dq-axis currents transient response. As presented in the control algorithm section, the q-axis current is related to the torque, so the transients of i_q are similar to T_e. While d-axis current is related to the flux control, both the torque and i_d have similar transients.

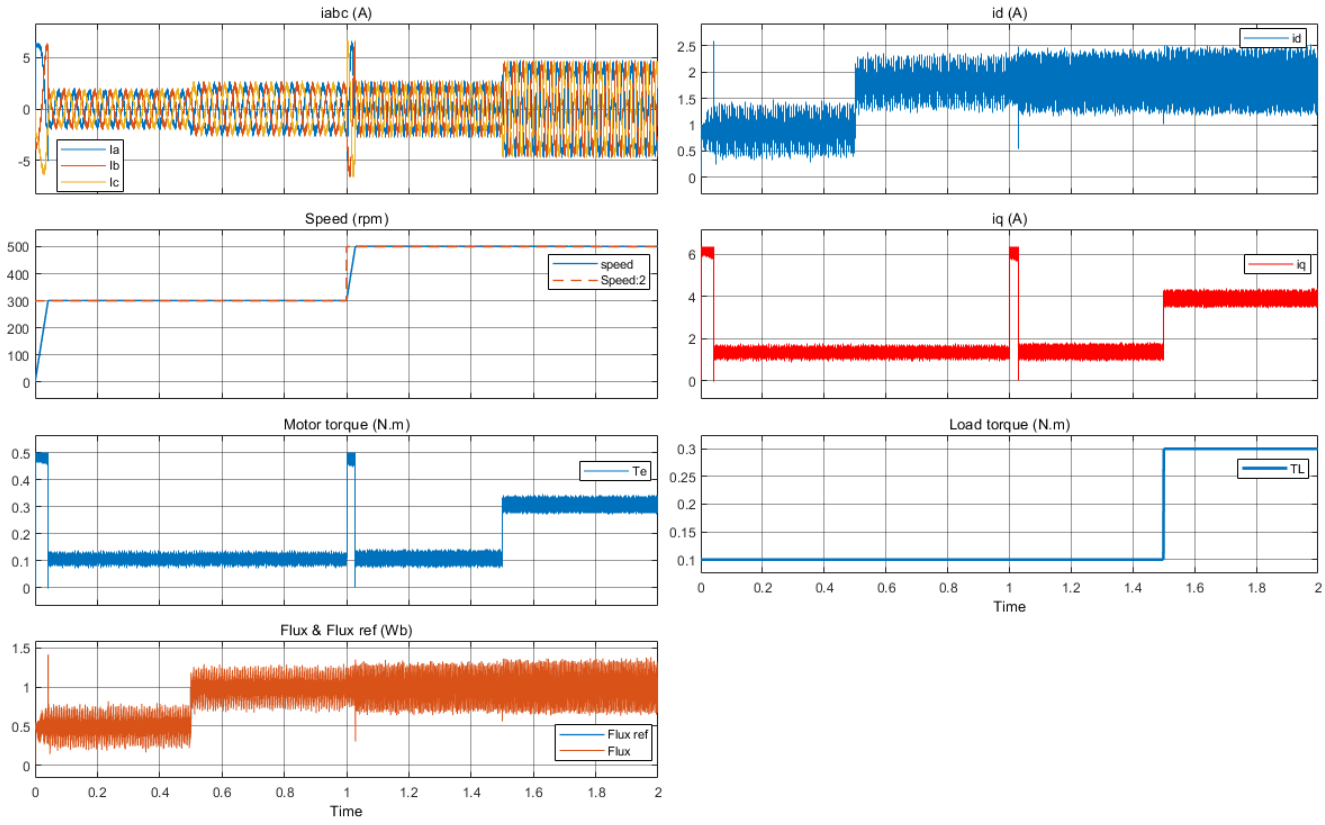

Figure 5. Simulation results of the overall performance of the PMSM.

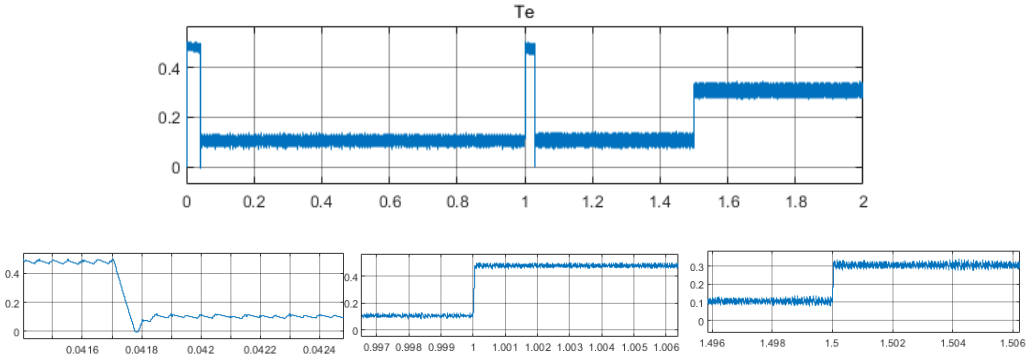

(**a**) The transient response of the electromagnetic torque

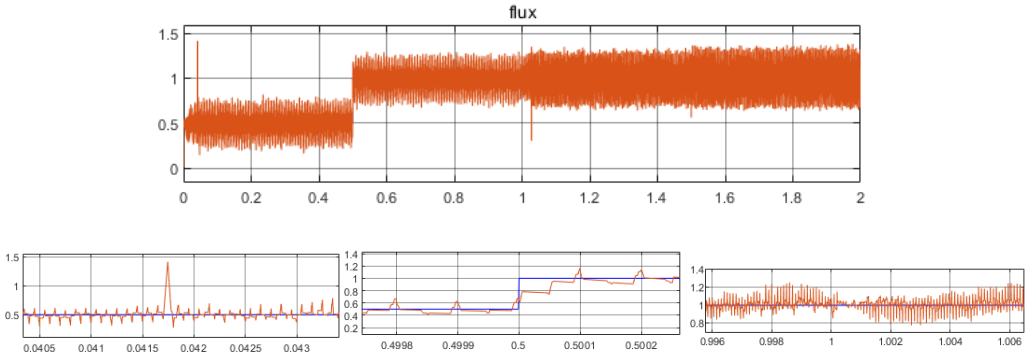

(**b**) Flux transient response

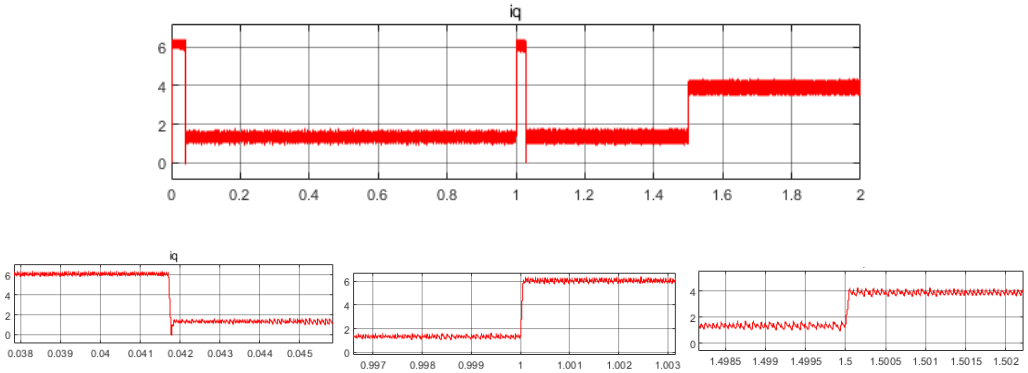

(**c**) The transient response of i_q

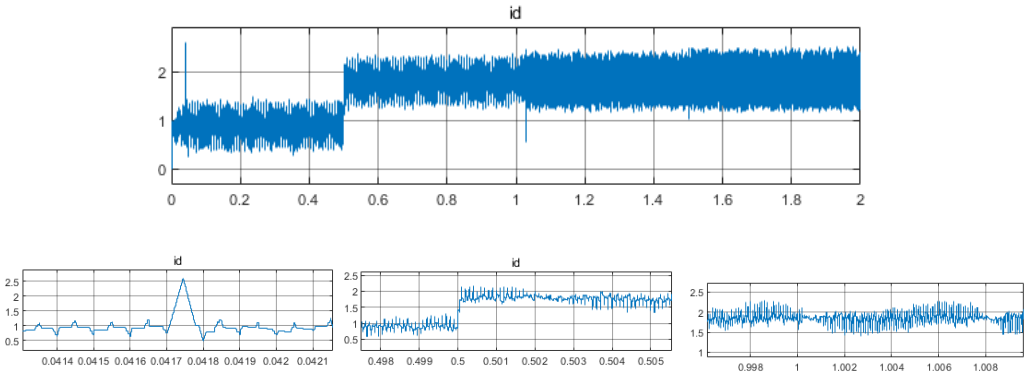

(**d**) The transient response of i_d

Figure 6. Transient response of the simulation results.

5. Experimental Analysis and Results

The experimental work was performed using a three-phase inverter board supplying a three-phase PMSM with 42 VDC. The three-phase inverter was controlled using a real-time interface platform, dSPACE DS1104. The experimental platform and system setup are shown in Figure 7.

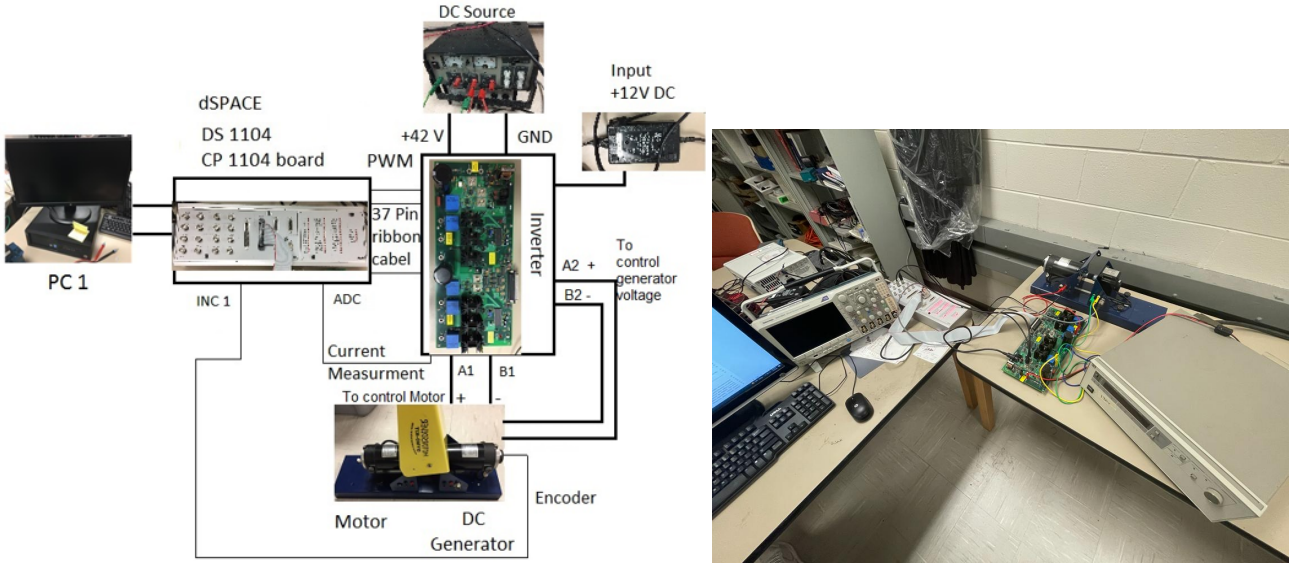

Figure 7. The experimental platform and system setup.

The experiment was conducted with the same PMSM parameters and the same controller gains listed in Tables 1 and 2, respectively. The experiment was conducted under three scenarios. In the first scenario, the speed was fixed and the flux was changed. In the second scenario, the flux was fixed, and the speed was changed. In the third scenario, the load torque was applied to the PMSM. The performance of the PMSM under these scenarios is presented.

5.1. Case 1: Speed Change

In this experiment, the reference flux was fixed as 0.5 Wb, and the reference speed was changed stepwise. The reference speed changed from 0 rpm to 300 RPM at $t = 2.28$ s. Then, it was changed to be 500 RPM at $t = 9.75$ s. The performance is presented in Figure 8. The speed controller tracked the reference speed correctly. However, changing the speed has no effect on the flux since they are controlled separately.

Figure 9 presents an expanded view of the motor during the steady state at constant reference speed and constant reference flux. The waveform of the current abc, the oscillatory steady-state error over the long run for the speed and the flux, and torque ripple that occurred for the PMSM can be observed from this figure.

The transient performance of the motor during the speed change from 300 rpm to 500 rpm at $t = 9.75$ s is shown in Figure 10.

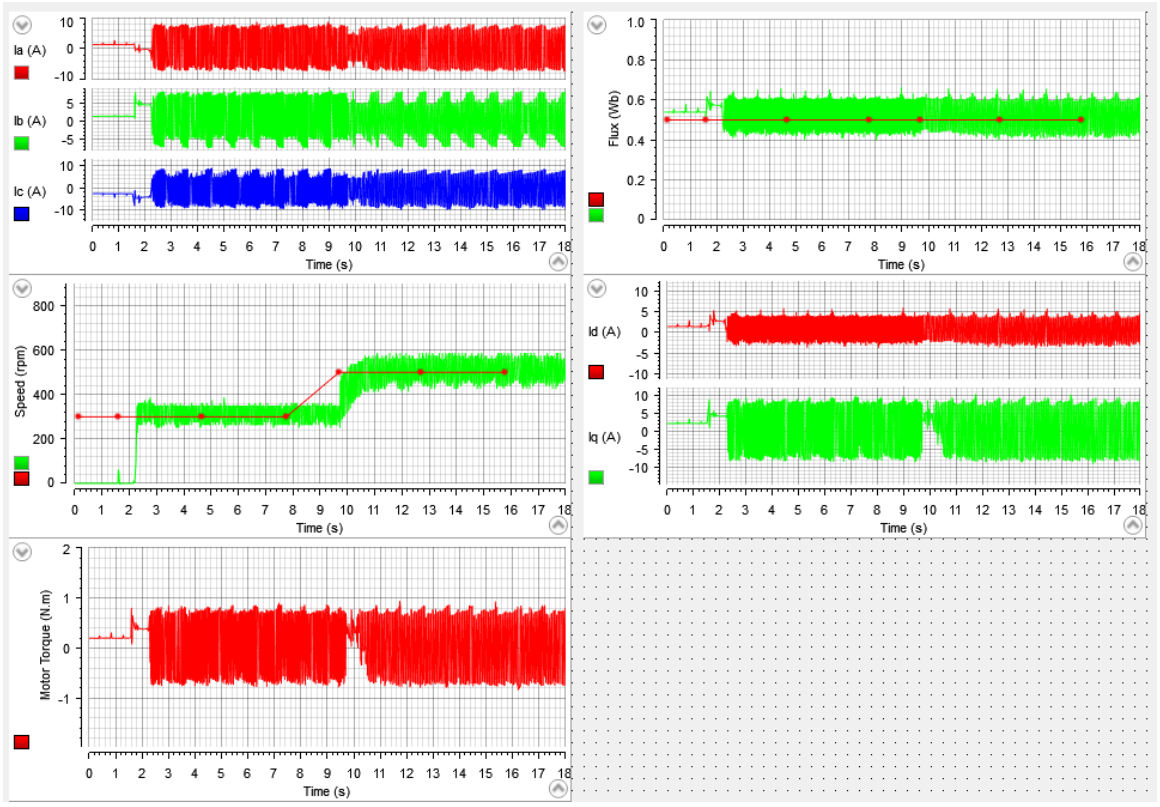

Figure 8. The PMSM performance at speed change.

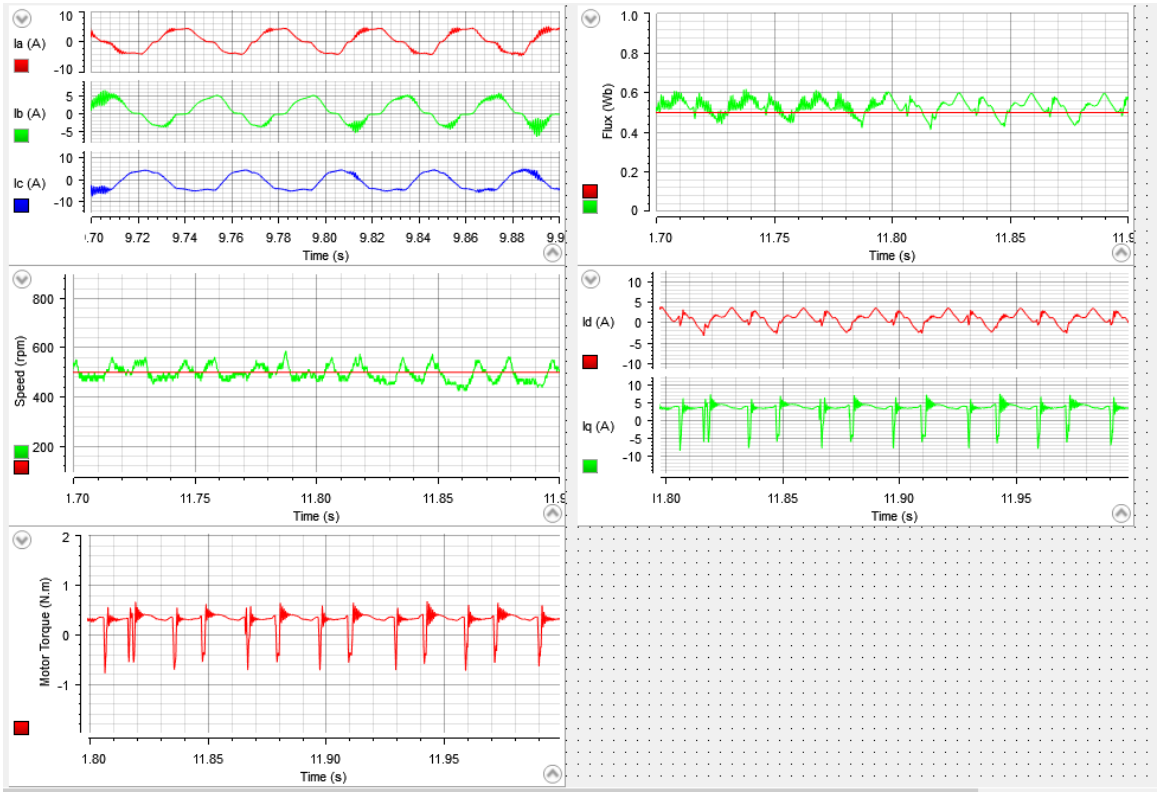

Figure 9. The PMSM performance during steady state.

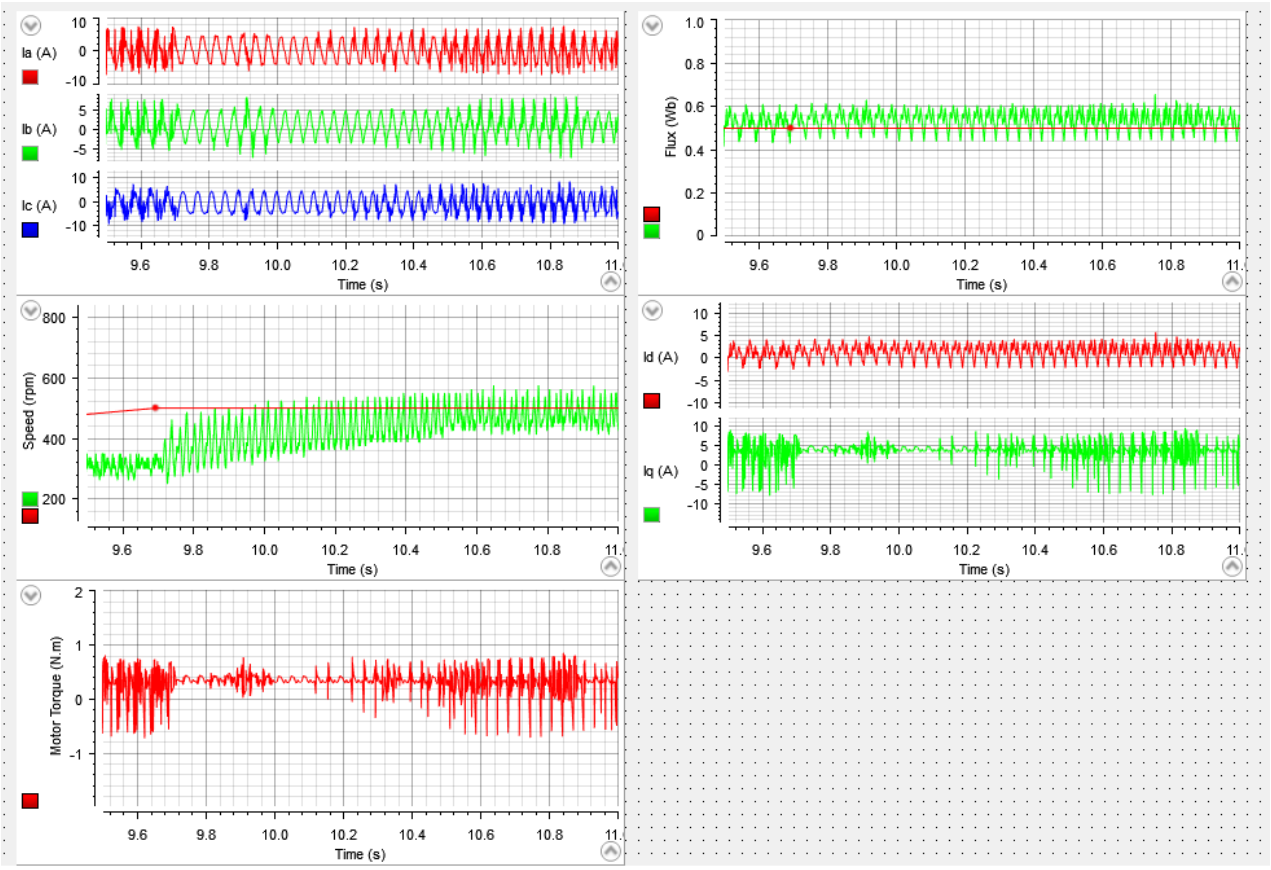

Figure 10. The transient PMSM performance at speed change.

5.2. Case 2: Flux Change

In this experiment, the reference speed of the PMSM was fixed as 500 rpm, and the reference flux was changed stepwise from 0 Wb to 0.75 Wb at $t = 5.1$ s and then to 1.5 Wb at $t = 10.9$ s. The hardware results are presented in Figure 11.

Because the speed and the flux are decoupled from each other, changing the flux has no effect on the motor speed, so the speed controller is able to maintain the motor speed as its reference value. In addition, the flux controller tracked the motor flux with some oscillation and controlled the d-axis reverence current. Based on the relationship between the flux and the d-axis reverence current, as shown in Equation (3), changing the flux will mainly affect i_d.

5.3. Case 3: Load Change

In this experiment, the reference flux and speed were fixed at 0.5 Wb and 500 RPM. The load was changed to be 0.2 N.m at $t = 13$ s. The experimental results are shown in Figure 12. The results prove that increasing the load torque on the motor does not affect either the speed or the flux controller behaviour.

The speed controller is still able to track the reference speed, and the flux controller is still able to track the reference flux as well without any changes. However, the oscillation of the motor torque response is increased. Hence, i_q and T_e are related; therefore, they have a similar response with different gains.

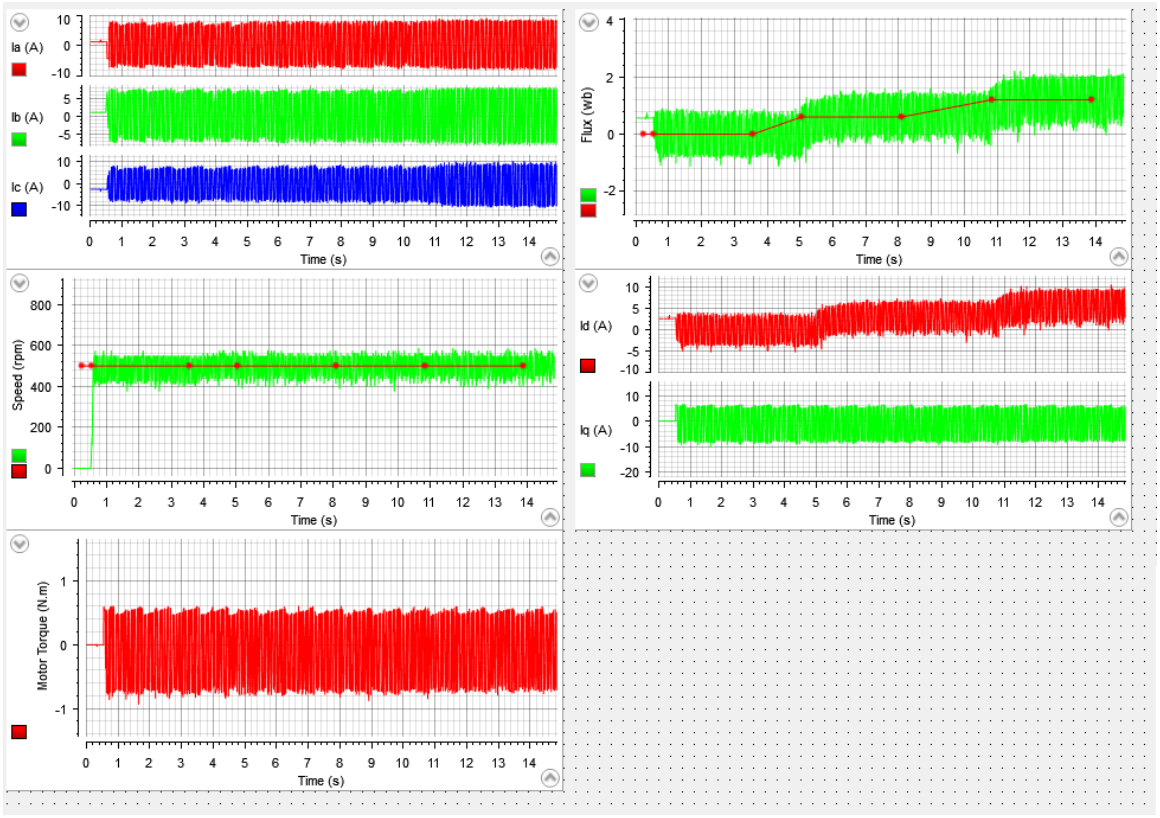

Figure 11. The PMSM performance at flux change.

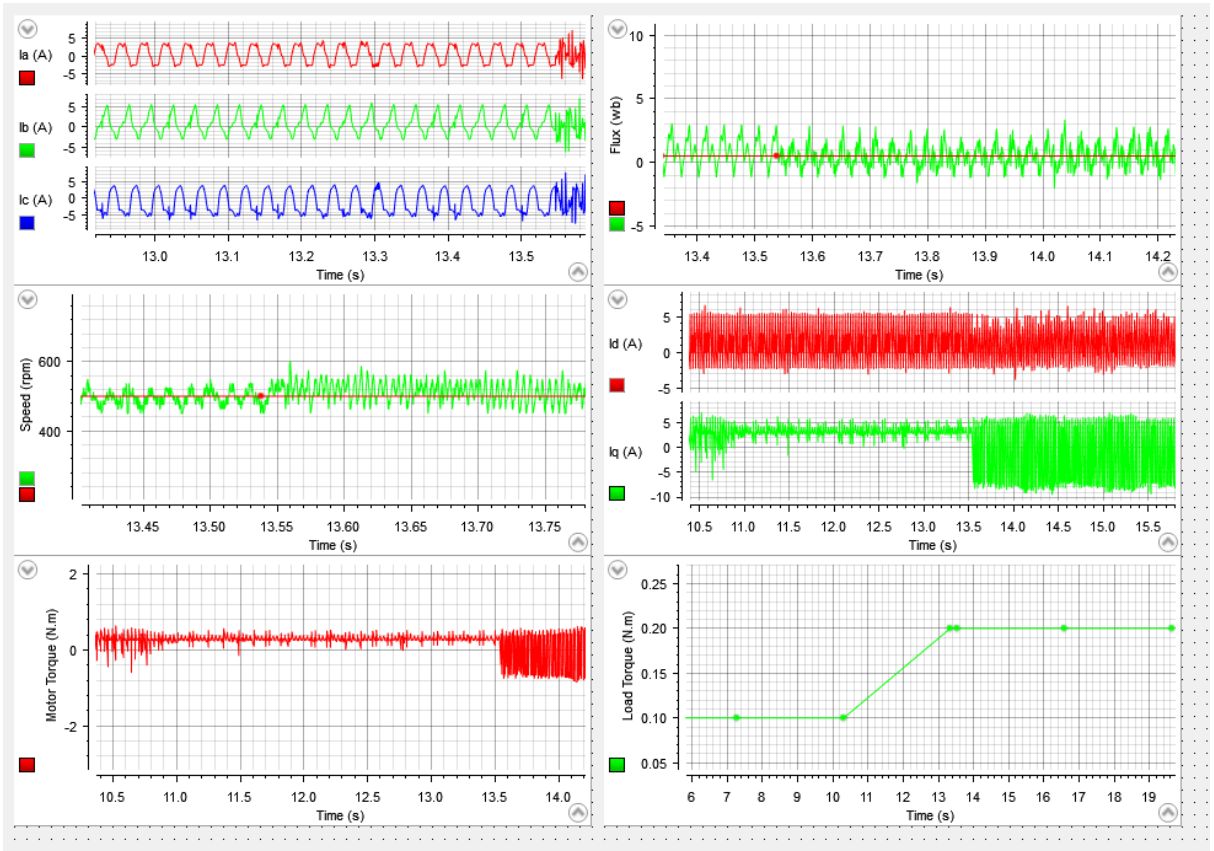

Figure 12. The PMSM performance at load change.

5.4. Limitations of This Study and the Shortcomings of the Proposed Method

The limitations of this study are in performing the hardware experiments in the flowing points. The sensor error and noise of the measurements created a large ripple in speed measurements and the flux and torque calculations as well. In the experiment, the load was a DC generator. This DC generator torque was controlled using the dSPACE DS1104 through an inverter. In performing the load change hardware experiment in Figure 12, the initial load was 0.1 N.m, then at time 10.5 s, the torque command was changed to 0.2 N.m. The torque controller needs time to reach its desired value. So, the three seconds load change existed because the controller needs time. The load is electrical and cannot be applied as input in the hardware. However, in the simulation, it is easy to add this change as a step input. Finally, the current control in performing the hardware experiments was limited to be between (−5 A, 5 A).

6. Conclusions

In this paper, a FOC scheme for a three-phase PMSM drive based on a decoupled flux and speed controller using the PR controller is presented. The FOC scheme allows the torque and the flux of the PMSM to be controlled separately. Furthermore, the design of the PR controller is included and proposed for the inner current loop. However, $dq0$ to $\alpha\beta0$ transformation is required to apply the PR control method.The proposed control method does not require torque and flux estimators, and no PLL is used, which reduces the overall complexity of the control system.

The simulation and hardware results show that the PMSM drive with the proposed control scheme has the merits of a simple control structure, robustness, fast motor response, and good performance. The performance of the PMSM was presented in three scenarios: flux change, speed change, and load torque change. As a result, both the flux and the speed of the PMSM were controlled separately under these scenarios.

Future work using a decoupled speed and flux controller based on the PR control method could be used and tested under open-circuit fault (OCF) conditions. The performance of the PMSM under the OCF based on the proposed control method could be tested under three case studies: flux change, speed change, and load change.In addition, a fault tolerance and fault detection methods can be applied under the same scenarios.

Author Contributions: Conceptualization, H.G., M.A., and R.M.N.; methodology, H.G.; software, H.G.; validation, H.G., M.A., and R.M.N.; formal analysis, H.G; investigation,H.G., M.A., and R.M.N.; supervision, R.M.N. All authors have read and agreed to the published version of the manuscript.

Funding: This research received no external funding.

Data Availability Statement: Not applicable.

Conflicts of Interest: The authors declare no conflict of interest.

Nomenclature

The following Nomenclature are used in this manuscript:

Rs	PMSM phase resistance
i_{abc}	Motor currents phases a , b, c
i_d	motor current d-axis component
i_q	motor current q-axis component
k_e	voltage constant of PMSM
k_i	integral component gain
k_p	proportional component gain
k_r	resonant component gain
k_t	torque constant
L_d	PMSM d-axis inductance

L_q	PMSM q-axis inductance
p	number of pole pairs
T_e	the electromagnetic torque
t	time
V_sd	The stator voltage of PMSM in d-axis
V_sq	The stator voltage of PMSM in q-axis
ψ_m	permanent magnetic flux linkage
ψ_{sd}	flux linkage of the stator in d-axis
ψ_{sq}	flux linkage of the stator in q-axis
θ_r	rotor angle position
ω	the fundamental angular frequency
ω_r	electrical rotor speed
ω_n	the natural frequency
ζ	the damping ratio

References

1. Ghanayem, H.; Alathamneh, M.; Nelms, R.M. A comparative study of PMSM torque control using proportional-integral and proportional-resonant controllers. In Proceedings of the SoutheastCon 2022, Mobile, AL, USA, 26 March–3 April 2022; pp. 453–458.
2. Stulrajter, M.; Hrabovcová, V.; Franko, M. Permanent Magnets Synchronous Motor Control Theory. *J. Electr. Eng.* **2007**, *58*, 79–84.
3. Sakunthala, S.; Kiranmayi, R.; Mandadi, P.N. A Review on Speed Control of Permanent Magnet Synchronous Motor Drive Using Different Control Techniques. In Proceedings of the International Conference on Power, Energy, Control and Transmission Systems (ICPECTS), Chennai, India, 22–23 February 2018; pp. 97–102.
4. Bida, V.M.; Samokhvalov, D.V.; Al-Mahturi, F.S. PMSM vector control techniques—A survey. In Proceedings of the IEEE Conference of Russian Young Researchers in Electrical and Electronic Engineering (EIConRus), Moscow/St. Petersburg, Russia, 29 January–1 February 2018; pp. 577–581.
5. Abassi, M.; Khlaief, A.; Saadaoui, O.; Chaari, A.; Boussak, M. Performance analysis of FOC and DTC for PMSM drives using SVPWM technique. In Proceedings of the 16th International Conference on Sciences and Techniques of Automatic Control and Computer Engineering (STA), Monastir,Tunisia, 21–23 December 2015; pp. 228–233.
6. Korkmaz, F.; Topaloğlu, I.; Çakir, M.F.; Gürbüz, R. Comparative performance evaluation of FOC and DTC controlled PMSM drives. In Proceedings of the 4th International Conference on Power Engineering, Energy and Electrical Drives, Istanbul, Turkey, 13–17 May 2013; pp. 705–708.
7. Dwivedi, S.; Singh, B. Vector Control vs. Direct Torque Control comparative evaluation for PMSM drive. In Proceedings of the Joint International Conference on Power Electronics, Drives and Energy Systems & 2010 Power India, New Delhi, India, 20–23 December 2010; pp. 1–8.
8. Yue, Y. ; Zhang, R.; Wu, B.; Shao, W. Direct torque control method of PMSM based on fractional order PID controller. In Proceedings of the 6th Data Driven Control and Learning Systems (DDCLS), Chongqing, China, 26–27 May 2017; pp. 411–415.
9. Gupta, N. P.; Gupta, P. Performance analysis of direct torque control of PMSM drive using SVPWM—Inverter. In Proceedings of the IEEE 5th India International Conference on Power Electronics (IICPE), Delhi, India, 6–8 December 2012; pp. 1–6.
10. Tang, M.; Zhuang, S. On Speed Control of a Permanent Magnet Synchronous Motor with Current Predictive Compensation. *Energies* **2019**, *12*, 65. [CrossRef]
11. Lyu, M.; Wu, G.; Luo, D.; Rong, F.; Huang, S. Robust Nonlinear Predictive Current Control Techniques for PMSM. *Energies* **2019**, *12*, 443. [CrossRef]
12. Codreş, B.; Găiceanu, M.; Şolea, R.; Eni, C. Model predictive speed control of Permanent Magnet Synchronous Motor. In Proceedings of the International Conference on Optimization of Electrical and Electronic Equipment (OPTIM), Bran, Romania, 22–24 May 2014; pp. 477–482.
13. Huang, X.; Pan, H.; Yuan, K. Speed and Current Control of PMSM based on Double MPC. In Proceedings of the 7th International Forum on Electrical Engineering and Automation (IFEEA), Hefei, China, 25–27 September 2020; pp. 300–304.
14. Fang, L.; Yushun, W.; Ruiqi, W. Simulation of speed-control system for PMSM based on sliding mode control. In Proceedings of the International Conference on Mechatronic Sciences, Electric Engineering and Computer (MEC), Shenyang, China, 20–22 December 2013; pp. 52–56.
15. Yan, L.; Dou, M.; Hua, Z. Disturbance Compensation-Based Model Predictive Flux Control of SPMSM with Optimal Duty Cycle. *IEEE Emerg. Sel. Top. Power Electron.* **2019**, *7*, 1872–1882. [CrossRef]
16. Mohamed, Y.A. A Novel Direct Instantaneous Torque and Flux Control With an ADALINE-Based Motor Model for a High Performance DD-PMSM. *IEEE Trans. Power Electron.* **2007**, *22*, 2042–2049. [CrossRef]
17. Dastjerdi, R. S.; Abbasian, M. A.; Saghafi, H.; Vafaie, M. H. Performance Improvement of Permanent-Magnet Synchronous Motor Using a New Deadbeat-Direct Current Controller. *IEEE Trans. Power Electron.* **2018**, *34*, 3530–3543. [CrossRef]
18. Rubino, S.; Bojoi, I.R.; Armando, E.; Tenconi, A. Deadbeat direct flux vector control of surface permanent magnet motor drives. *IEEE Trans. Ind. Appl.* **2020**, *56*, 2685–2699. [CrossRef]

19. Dai, S.; Wang, J.; Sun, Z.; Chong, E. Deadbeat predictive current control for high-speed PMSM drives with low switching-to-fundamental frequency ratios. *IEEE Trans. Ind. Electron.* **2021**, *69*, 4510–4521. [CrossRef]
20. Sun, X.; Zhang, Y.; Lei, G.; Guo, Y.; Zhu, J. An improved deadbeat predictive stator flux control with reduced-order disturbance observer for in-wheel PMSMs. *IEEE/ASME Trans. Mechatron.* **2021**, *27*, 690–700 [CrossRef]
21. Chen, J.; Wang, J.; Yan, B. Simulation Research on Deadbeat Direct Torque and Flux Control of Permanent Magnet Synchronous Motor. *Energies* **2022**, *15*, 3009. [CrossRef]
22. Yun, D.; Kim, N.; Hyun, D.; Baek, J. Torque Improvement of Six-Phase Permanent-Magnet Synchronous Machine Drive with Fifth-Harmonic Current Injection for Electric Vehicles. *Energies* **2022**, *15*, 3122. [CrossRef]
23. Ton, T.-D.; Hsieh, M.-F. A Deadbeat Current and Flux Vector Control for IPMSM Drive with High Dynamic Performance. *Appl. Sci.* **2022**, *12*, 3789. [CrossRef]
24. Zhang, K.; Xie, Y.; Li; S.; He, Y. Vector Control of PMSM Based on Proportional Resonance Control. In Proceedings of the 6th Inter-national Conference on Systems and Informatics (ICSAI), Shanghai, China, 2–4 November 2019; pp. 51–56.
25. Minghe, T.; Bo, W.; Yong, Y.; Xing, M.; Qinghua; D.; Dianguo, X. Proportional Resonant-Based Active Disturbance Rejection Control for Speed Fluctuation Suppression of PMSM Drives. In Proceedings of the 22nd International Conference on Electrical Machines and Systems (ICEMS), Harbin, China, 11–14 August 2019; pp. 1–6.
26. Vujji; A.; Dahiya, R. Speed Estimator for Direct Torque and Flux Control of PMSM Drive using MRAC based on Rotor flux. In Proceedings of the IEEE 9th Power India International Conference (PIICON), Sonepat, India, 28 February–1 March 2020; pp. 1–6.
27. Yunhao, P.; Dejun, Y., Yansong, H. The stator flux linkage adaptive SVM-DTC control strategy of permanent magnet synchronous motor. In Proceedings of the 6th Asia Conference on Power and Electrical Engineering (ACPEE), Chongqing, China, 8–11 April 2021; pp. 826–831.
28. Krause, P.C.; Wasynczuk, O.; Sudhoff, S.D.; Pekarek, S.D. *Analysis of Electric Machinery and Drive Systems*; Wiley-IEEE Press: Piscatawy, NJ, USA, 2013.
29. Ziegler, J.G.; Nichols, N.B. Optimum Settings for Automatic Controllers. *J. Dyn. Syst. Meas. Control* **1993**, *115*, 220–222. [CrossRef]
30. Alathamneh, M.; Ghanayem, H.; Yang, X.; Nelms, R.M. Three-Phase Grid-Connected Inverter Power Control under Unbalanced Grid Conditions Using a Proportional-Resonant Control Method. *Energies* **2022**, *15*, 7051. [CrossRef]
31. Holmes, D.G.; Lipo, T.A.; McGrath, B.P.; Kong, W.Y. Optimized Design of Stationary Frame Three Phase AC Current Regulators. *IEEE Trans. Power Electron.* **2009**, *24*, 2417–2426. [CrossRef]